Acc. Chem. Res. **2001,** *34,* 40−48

Mimicking Photosynthetic Solar Energy Transduction

DEVENS GUST,* THOMAS A. MOORE,* AND ANA L. MOORE*

Department of Chemistry and Biochemistry, Center for the Study of Early Events in Photosynthesis, Arizona State University, Tempe, Arizona 85287

Received May 23, 2000

ABSTRACT

Increased understanding of photosynthetic energy conversion and advances in chemical synthesis and instrumentation have made it possible to create artificial nanoscale devices and semibiological hybrids that carry out many of the functions of the natural process. Artificial light-harvesting antennas can be synthesized and linked to artificial reaction centers that convert excitation energy to chemical potential in the form of long-lived charge separation. Artificial reaction centers can form the basis for molecular-level optoelectronic devices. In addition, they may be incorporated into the lipid bilayer membranes of artificial vesicles, where they function as components of light-driven proton pumps that generate transmembrane proton motive force. The proton gradient may be used to synthesize adenosine triphosphate via an ATP synthase enzyme. The overall energy transduction process in the liposomal system mimics the solar energy conversion system of a photosynthetic bacterium. The results of this research illustrate the advantages of designing functional nanoscale devices based on biological paradigms.

Introduction

Sunlight is absorbed and converted to electronic excitation energy, which initiates a chain of electron-transfer events leading to charge separation across a photosynthetic membrane. The resulting potential energy is used to pump protons across the membrane, generating an osmotic and charge imbalance which in turn powers the synthesis of adenosine triphosphate (ATP), a high-energy biological fuel. This improbable approach to solar energy conversion is a prime example of the Rube Goldberg designs common[1] in biological systems. However, it and related photosynthetic processes power life as we know it and have done so successfully for several billions of years.

The success of photosynthesis prompts research on the natural process and spurs attempts to emulate it in the laboratory. Biomimetic systems, which reduce the complicated natural mechanism to its basic elements, can lead to a better understanding of photosynthesis and to artificial power sources for biological processes. Potential applications of artificial photosynthesis to solar energy conversion have been discussed for a century.[2] More recently, it has been recognized that artificial photosynthesis research also has potential uses in molecular-scale optoelectronics, photonics, sensor design, and other areas of nanotechnology.

There are many approaches to the application of the basic physical and chemical principles of photosynthesis to artificial systems.[3−7] Here, the focus is on recent research from our laboratories. We will begin with a short primer on the natural process and then consider biomimicry.

Natural Photosynthesis in Bacteria

Solar energy conversion in purple bacteria has much in common with its analogue in green plants but is simpler and better understood. It is a cyclic process, lacking the complications of two photosystems and water oxidation. For these reasons, we chose it as a model for biomimicry. Figure 1 shows the relevant steps, which occur in or across a lipid bilayer membrane and are mediated by membrane-bound proteins.

Photosynthesis runs on visible and near-infrared photons. The light is collected by antenna systems tuned to maximize use of wavelengths available in the habitat of the organism. Electronic excitation in the antenna migrates from chromophore to chromophore and ultimately to a reaction center, where it is converted to chemical energy in the form of charge separation across the bilayer. This occurs when photoinduced electron transfer from an excited bacteriochlorophyll "special pair" near the external side of the plasma membrane initiates transmission of an electron across the membrane in a series of steps involving several donor−acceptor cofactors. The ultimate electron acceptor, a quinone molecule, is reduced to a semiquinone and finally to a hydroquinone after two photoinduced electron transfers. This reduction involves the uptake of two protons from water on the internal, cytoplasmic side of the membrane. The hydroquinone diffuses to the next component of the apparatus, a proton pump, labeled the cytochrome bc_1 complex in Figure 1. This complex oxidizes the hydroquinone back to a quinone, using the energy released to translocate protons across the membrane and establish a proton concentration and charge imbalance (proton motive force, pmf). The oxidation process is ultimately driven, via various cytochrome redox relays, by the oxidized special pair, which becomes reduced to its initial state. Finally, the enzyme ATP synthase allows protons to flow back across the mem-

Devens Gust, born in Phoenix, AZ, on November 28, 1944, received his B.S. in chemistry from Stanford University and his Ph.D. from Princeton University. After a year of postdoctoral work at Caltech, he accepted a faculty position at Arizona State University. He is currently Professor and Chair, Department of Chemistry and Biochemistry at ASU.

Thomas A. Moore was born in Pensacola, FL, on June 3, 1944. After receiving the B.A. and Ph.D. degrees in chemistry from Texas Tech University, he spent three years as a postdoctoral associate at the University of Washington. In 1976, he joined Arizona State University, where he is now Professor of Biochemistry.

Ana L. Moore was born April 14, 1942, in Buenos Aires, Argentina. She received a Bachelor of Pharmacy degree at the Universidad Nacional de La Plata, Argentina, and the M.S. in chemistry from the Universidade Federal do Rio de Janeiro, Brazil, before coming to Texas Tech University, where she was awarded the Ph.D. in chemistry. After spending three years as a postdoctoral associate at the University of Washington, she moved to Arizona State University, where she is currently Professor of Chemistry.

10.1021/ar9801301 CCC: $20.00
Published on Web 11/08/2000

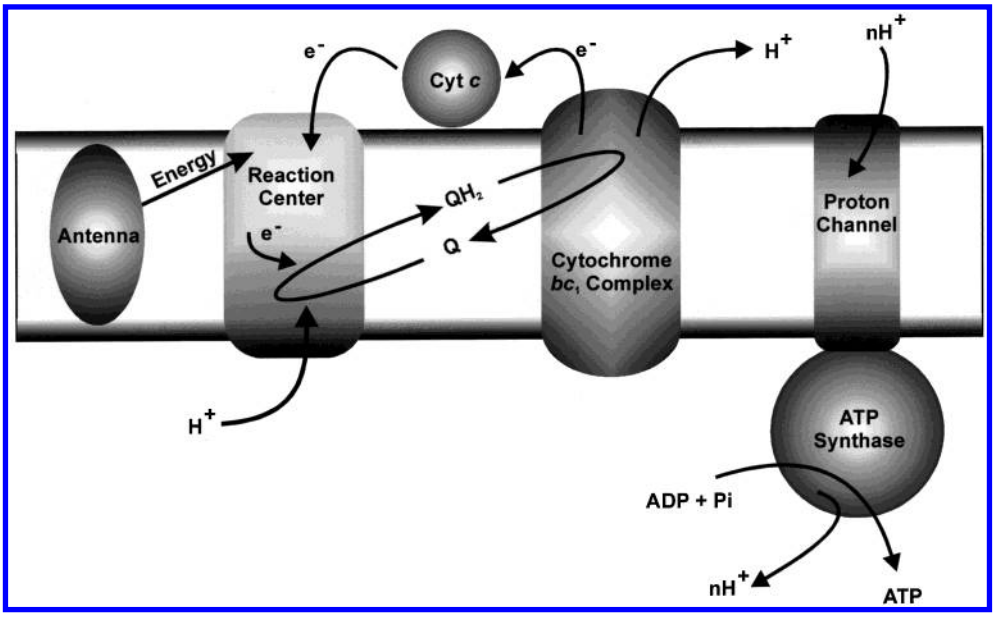

FIGURE 1. Bacterial photosynthetic membrane. The horizontal band represents the lipid bilayer containing the various protein components. Photosynthesis begins with light absorption by the antenna and culminates in the production of ATP.

Chart 1

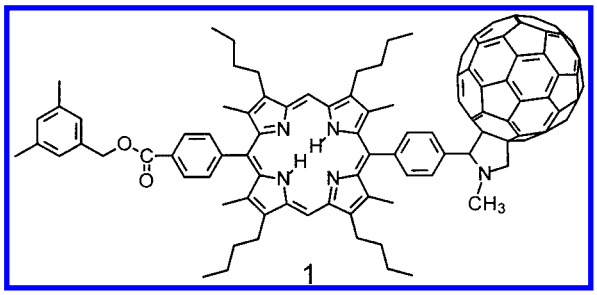

1

brane, down the thermodynamic gradient, driving the release of ATP formed from adenosine diphosphate and inorganic phosphate (Pi). The ATP fills the majority of the energy needs of the bacterium.

Artificial Photosynthesis

Artificial Reaction Centers. What are the design requirements for an artificial reaction center? As its basic operation is photoinduced electron transfer, a model reaction center must at minimum consist of an electron donor (or acceptor) chromophore that absorbs visible light, an additional electron acceptor (or donor) moiety, and an organizational principle that controls their electronic interactions (and therefore the rates and yields of electron transfer). Molecular dyad **1** (Chart 1) is an example.[8] The porphyrin (P) is a model for the less stable and less synthetically tractable chlorophyll. The fullerene (C_{60}) functions as an electron acceptor. The covalent linkage joining the two moieties provides electronic coupling that allows photoinduced electron transfer to compete with the usual photophysical pathways that depopulate excited states.

The photochemistry of the dyad in 2-methyltetrahydrofuran solution has been unraveled using transient spectroscopic techniques.[8] Excitation of the porphyrin gives the first excited singlet state, ^{1}P-C_{60}, which decays by photoinduced electron transfer to yield $P^{\bullet+}$-$C_{60}^{\bullet-}$ with a rate constant of 3.3×10^{11} s^{-1}. This rate constant is substantially larger than those for competing processes such as fluorescence, internal conversion, intersystem crossing, and energy transfer to the fullerene, and the quantum yield of $P^{\bullet+}$-$C_{60}^{\bullet-}$ is unity. Based on cyclic voltammetric measurements, the charge-separated state lies ~1.39 eV above the ground state (and 0.58 eV below ^{1}P-C_{60} at 1.97 eV). It therefore stores a significant fraction of the photon energy as chemical potential. Thus, dyad **1** would seem to be an excellent mimic for the reaction center. However, $P^{\bullet+}$-$C_{60}^{\bullet-}$ decays back to the ground state by charge recombination with a lifetime of 478 ps. This short time precludes facile harvesting of the stored energy.

All dyad-type artificial reaction centers suffer to a greater or lesser extent from rapid charge recombination. In 1983, we developed a biomimetic solution to this problem.[9,10] In photosynthesis, long-lived charge separation is ensured by the large distance between the special pair and the final quinone acceptor, which leads to weak electronic coupling and slow charge recombination. The weak coupling also makes photoinduced electron transfer from the special pair to the final quinone in a single step undetectably slow. A high quantum yield of charge separation is ensured by forming the final state via a series of short-range, fast, and efficient electron transfers. An electron hops from the excited special pair, via a bacteriochlorophyll, to a bacteriopheophytin. A subsequent transfer moves an electron to an initial quinone, and the last step transports the charge to the ultimate quinone acceptor. This strategy was exploited in a triad employing two electron donors and one acceptor, in which two sequential electron transfers lead to long-lived charge separation.[9,10]

Triad **2** (Chart 2) is a modern embodiment of this approach.[11] It consists of a porphyrin bearing a fullerene, as in **1**, and a carotenoid (C) secondary electron donor.

Chart 2

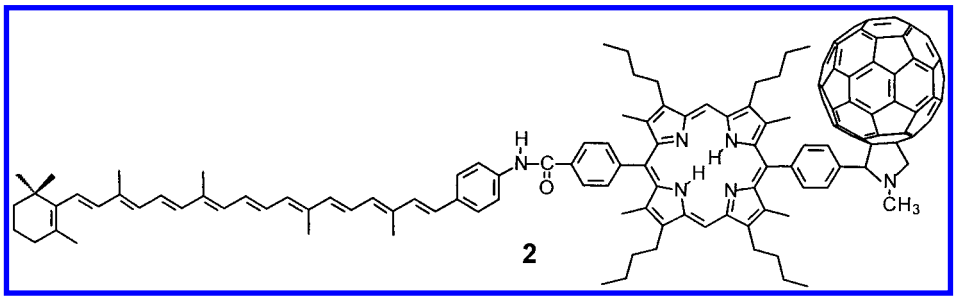

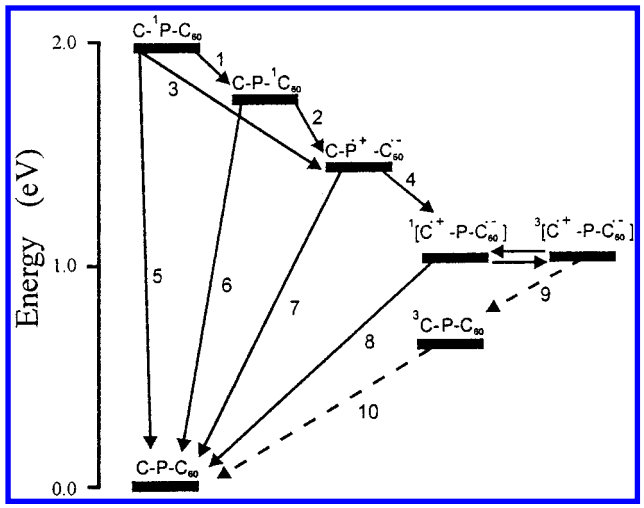

FIGURE 2. High-energy states and interconversion pathways for C-P-C_{60} triad artificial reaction center **2**. The energies of the charge-separated states are estimated from electrochemical studies in polar solvents, and the energies of the excited states are derived from spectroscopic properties.

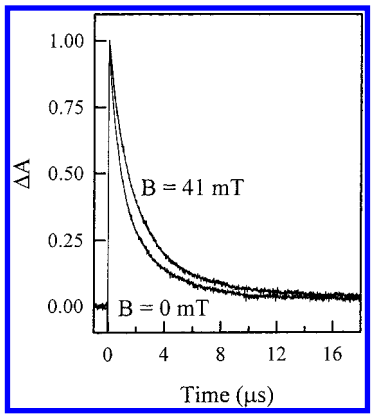

FIGURE 3. Decay of the $C^{\bullet+}$-P-$C_{60}^{\bullet-}$ state of **2** in a 2-methyltetrahydrofuran glass at 77 K, detected via the transient absorbance at 980 nm. The lifetime of the state increases by a factor of 1.5 in the presence of a 41-mT magnetic field.

Excitation of a 2-methyltetrahydrofuran solution of **2** is followed by the events diagrammed in Figure 2. Decay of C-^{1}P-C_{60} by photoinduced electron-transfer step 3 gives C-$P^{\bullet+}$-$C_{60}^{\bullet-}$, with $k_3 = 3.3 \times 10^{11}$ s^{-1} and a quantum yield of unity. (Although not populated significantly in this particular experiment, C-P-$^1C_{60}$ also decays to C-$P^{\bullet+}$-$C_{60}^{\bullet-}$ by electron transfer.) As deduced from dyad **1**, C-$P^{\bullet+}$-$C_{60}^{\bullet-}$ can return to the ground state by a charge recombination step 7 ($k_7 = 2.1 \times 10^9$ s^{-1}). Because the molecule is a triad, electron transfer from the carotenoid to the porphyrin (step 4, $k_4 = 1.5 \times 10^{10}$ s^{-1}) competes with recombination to yield $C^{\bullet+}$-P-$C_{60}^{\bullet-}$. This state is produced with an overall quantum yield of 0.88. It decays slowly by charge recombination, step 9, to yield the carotenoid triplet ($k_9 = 2.9 \times 10^6$ s^{-1}). Thus, the two-step electron-transfer sequence in triad **2** has increased the lifetime of charge separation by a factor of nearly 1000, relative to dyad **1**.

Triad **2** is an example of a successful artificial reaction center that uses visible light to produce a long-lived, energetic charge-separated state in high quantum yield. Triad **2** and related triads demonstrate several types of behavior that are also found in reaction centers but are much less common in biomimetic systems.[11−16] For example, formation of $C^{\bullet+}$-P-$C_{60}^{\bullet-}$ occurs even in a glass at 8 K. The initial steps of photosynthesis persist at 4 K, but photoinduced electron transfer in most model systems ceases at low temperature when the solvent becomes glassy. Charge recombination of $C^{\bullet+}$-P-$C_{60}^{\bullet-}$ yields ^{3}C-P-C_{60} with a unique EPR-detectable spin polarization pattern and occurs by a radical pair mechanism,[12] as observed in natural reaction centers.[17−19]

These triads also exhibit the transfer of triplet excitation energy by a relay mechanism related to that found in some reaction centers.[14] In toluene, the C-P-$^1C_{60}$ state of **2** does not undergo electron transfer, decaying instead by intersystem crossing to yield C-P-$^3C_{60}$. This triplet decays with a time constant of 110 ns to give the carotenoid triplet. Formation of ^{3}C-P-C_{60} occurs by a two-step process. The C-P-$^3C_{60}$ is converted to C-^{3}P-C_{60} by relatively slow, endergonic triplet−triplet energy transfer. The intermediate C-^{3}P-C_{60} rapidly forms the carotenoid triplet. In nature, the quenching of chlorophyll triplets by carotenoids is an important photoprotective mechanism through which photosynthetic organisms avoid light-induced damage due to chlorophyll-sensitized singlet oxygen formation.

An Optomagnetic Molecular Switch. The unusual recombination of $C^{\bullet+}$-P-$C_{60}^{\bullet-}$ in C-P-C_{60} triads to yield the carotenoid triplet also makes it possible to control the lifetime of $C^{\bullet+}$-P-$C_{60}^{\bullet-}$ using magnetic fields.[16] Figure 3 shows the decay of the transient absorbance of the $C^{\bullet+}$-P-$C_{60}^{\bullet-}$ state of a triad closely related to **2** in a 2-methyltetrahydrofuran glass at 77 K. When a small magnetic field of 41 mT is applied, the lifetime of the charge-separated state is increased by a factor of 1.5. The explanation is that $C^{\bullet+}$-P-$C_{60}^{\bullet-}$ is produced as a singlet biradical, but due to the long lifetime and the weak coupling between the electrons, the biradical equilibrates among the essentially isoenergetic singlet and three triplet

Chart 3

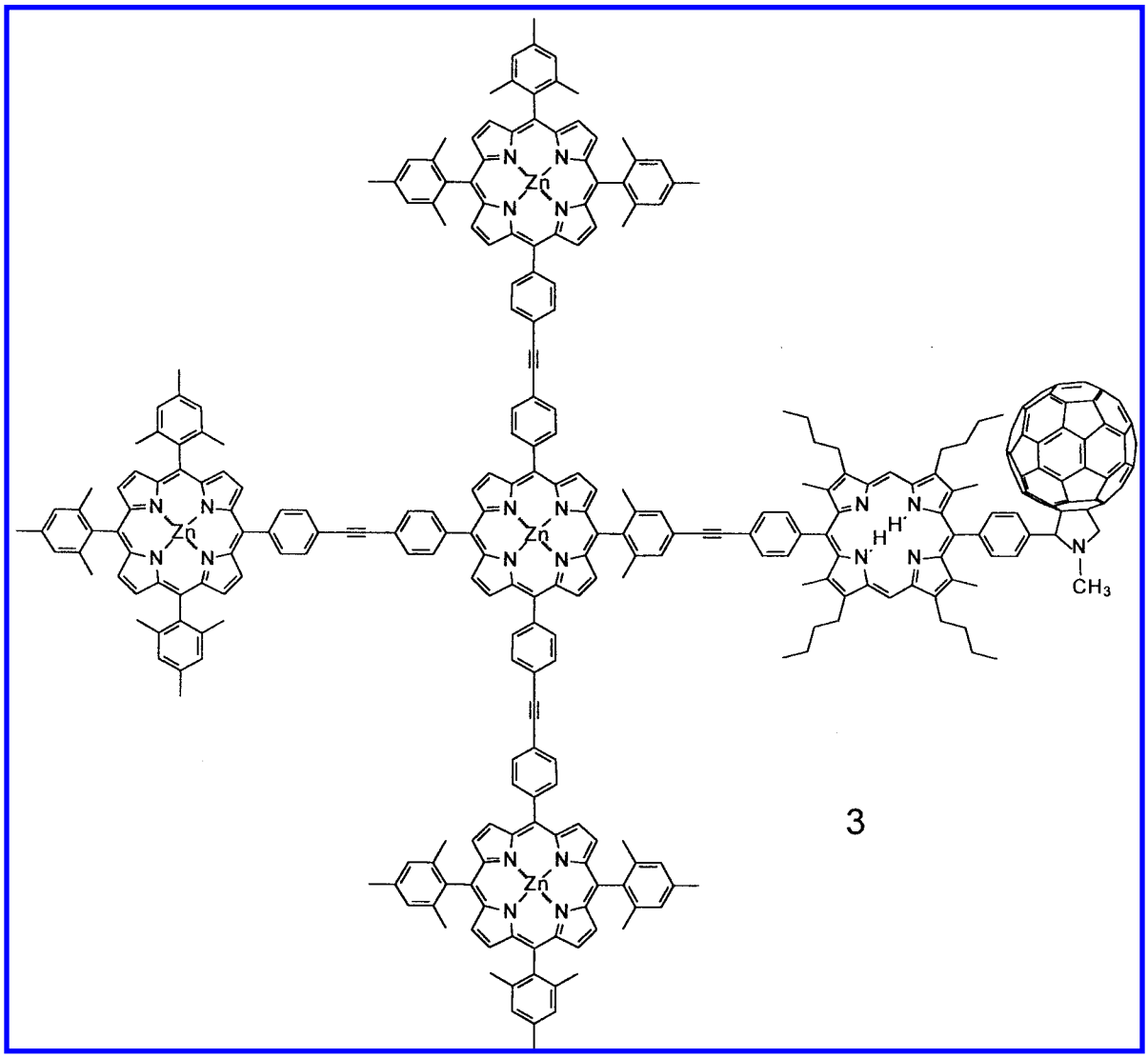

sublevels. Only the triplet sublevels, which contain three-fourths of the total population, may recombine to yield the carotenoid triplet. In principle, the singlet biradical could recombine to the ground state, but this is slow due to unfavorable thermodynamics.[16] In the presence of the magnetic field, the energies of two of the triplet sublevels, T_+ and T_-, are split away from those of the singlet and T_0 states by the Zeeman interaction and are no longer populated. The biradical population now equilibrates between the singlet and T_0 states. Therefore, only half of the total biradical population can recombine to yield ^{3}C-P-C_{60}, giving rise to the factor of 1.5 in lifetime.

The triad may be thought of as a molecular-scale AND logic gate. The gate has two inputs: light and magnetic field. When just the light pulse is supplied, only the shorter-lived charge-separated state is produced. When just the magnetic field is applied, no charge separation is observed. Only when both the light pulse and the magnetic field are applied is the longer-lived charge separation achieved. This is the behavior required by an AND gate, which switches its output state only when both of its two inputs are "on". Although the magnitude of the magnetic field effect is not large in an absolute sense, the output of triad gate **2** can be detected with a high signal-to-noise ratio by integration of the transient absorbance of the carotenoid radical cation.[16]

Incorporation of Artificial Antennas. Recent advances in understanding photosynthetic antennas and improvements in synthetic and spectroscopic methods have allowed development of artificial light-harvesting antennas that absorb light and rapidly transfer excitation among various component chromophores.[20] For example, synthetic porphyrins may be linked to form antenna arrays and photonic "wires", gates, and switches.[21−23] Recently, an artificial antenna array has been linked to an artificial reaction center to form a functional unit.[24] The antenna of $(P_{ZP})_3$-P_{ZC}-P-C_{60} hexad **3** (Chart 3) comprises four zinc tetraarylporphyrins, $(P_{ZP})_3$-P_{ZC}, which are joined to a free base porphyrin−fullerene artificial reaction center analogous to **1** (P-C_{60}). As revealed by time-resolved spectroscopy, excitation of any peripheral zinc porphyrin moiety (P_{ZP}) in 2-methyltetrahydrofuran is followed by energy transfer to the central zinc porphyrin to give $(P_{ZP})_3$-$^1P_{ZC}$-P-C_{60} with a time constant of 50 ps. The excitation

Chart 4

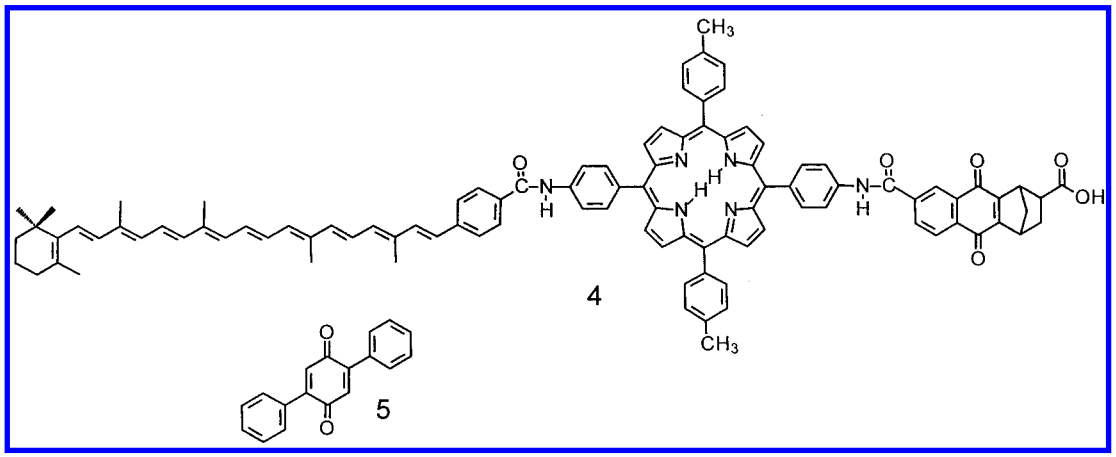

migrates to the free base porphyrin in 240 ps to yield $(P_{ZP})_3$-P_{ZC}-^{1}P-C_{60}, which decays by electron transfer to the fullerene with a time constant of 3 ps. The resulting $(P_{ZP})_3$-P_{ZC}-$P^{\bullet+}$-$C_{60}^{\bullet-}$ state has a lifetime of 1.3 ns and is generated with a quantum yield of 0.70.

Complex **3** mimics the basic functions of both photosynthetic antennas and reaction center complexes. In the future, antenna−reaction center models will feature larger light-harvesting arrays, higher quantum yields for charge separation, longer lifetimes for the charge-separated states, and possibly more energetic charge-separated states. Both self-assembly and dendritic-type syntheses seem promising ways to prepare very large artificial antennas.

A Light-Driven Transmembrane Proton Pump. As illustrated above, artificial photosynthetic reaction centers are now a reality. As suggested by Figure 1, a logical next step in the evolution of artificial photosynthesis is to use such centers to power transmembrane proton pumps. This has now been accomplished.[25] The pump comprises carotenoid−porphyrin−quinone (C-P-Q) triad **4** and quinone **5** (Chart 4). These molecules are housed in the lipid bilayer membrane of a liposome vesicle with a diameter of ∼150 nm (Figure 4). The triad is inserted vectorially into the membrane so that the majority of the molecules have the quinone near the external surface. This asymmetry is achieved by preforming the vesicles and then introducing the triad dissolved in a small amount of tetrahydrofuran into the solution. As the organic solvent dissipates, the water-insoluble triads dissolve into the membrane. The hydrophobic carotenoid portion can enter the hydrophobic core of the membrane, but the quinone moiety, which bears a negatively charged carboxylate group, remains near the hydrophilic exterior. Quinone **5** is soluble only in the hydrophobic membrane interior and has a higher reduction potential than the naphthoquinone moiety of the triad.

The pump is based on a redox loop.[26] It is powered by the triad which, upon absorption of light by the porphyrin, generates a $C^{\bullet+}$-P-$Q^{\bullet-}$ charge-separated state by a mechanism similar to that shown in Figure 2. Although all details of the function of the pump have not been elucidated, the following description illustrates the major

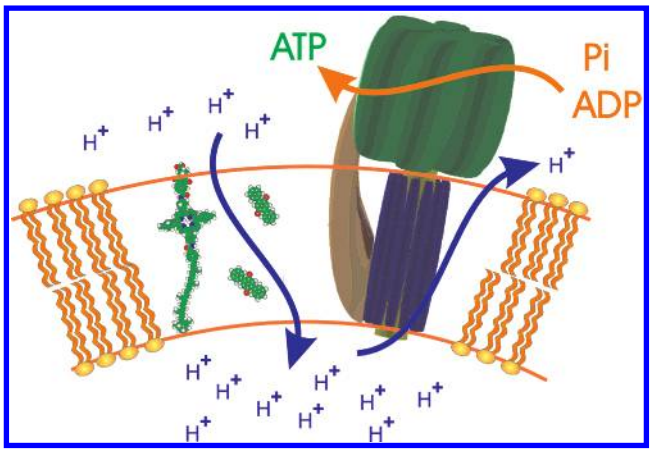

FIGURE 4. Schematic representation of an artificial photosynthetic membrane. The lipid bilayer of a liposome vesicle contains the components of a light-driven proton pump: a vectorially inserted C-P-Q triad molecule **4** and "shuttle" quinone **5**. Illumination of the triad leads to transport of hydrogen ions into the liposome interior, establishing a proton motive force. The membrane also contains a vectorially inserted ATP synthase enzyme. The flow of protons out of the liposome through this enzyme drives the production of ATP.

aspects of the process. The quinone radical anion of $C^{\bullet+}$-P-$Q^{\bullet-}$ near the outer membrane surface reduces a molecule of quinone **5** to yield the semiquinone anion, which is basic enough to accept a proton from the exterior aqueous environment. The resulting neutral semiquinone radical diffuses within the bilayer. When it encounters the carotenoid radical cation near the inner membrane surface, it is oxidized back to the quinone. The protonated quinone is a strong acid ($pK_a \approx -6$) that releases the proton into the inner volume of the liposome. The net result is proton translocation into the vesicle interior and regeneration of the photoredox catalyst. The redox loop-based proton pump can, in principle, be driven from various combinations of redox levels of quinone **5**.

The action of this pump will acidify the solution inside the liposome but will have little effect on the pH of the much larger exterior volume. Therefore, characterization of the pump requires a method for detecting a transmembrane proton gradient. This can be done using a pH-sensitive fluorescent dye such as pyranine trisulfonate. When this material is dissolved in the water inside the

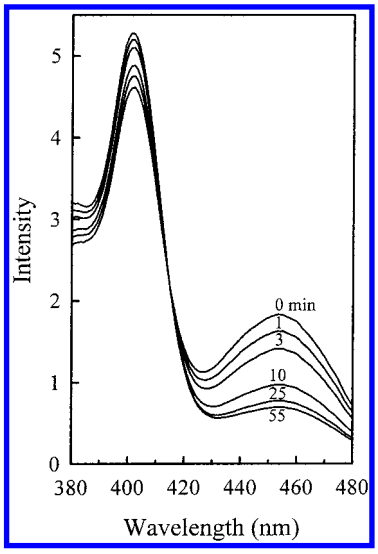

FIGURE 5. Light-driven proton pumping as detected by the fluorescence excitation spectrum of the pH-sensitive dye pyranine-trisulfonate. Illumination of the liposomal system leads to acidification of the inside of the liposome and protonation of the dye. This causes a decrease in the excitation band at 456 nm and a corresponding increase at 406 nm.

liposomes, it reports the pH via the ratio of amplitudes of its fluorescence excitation spectrum at 406 and 456 nm. Figure 5 shows the results of a typical experiment. Irradiation with light absorbed by the porphyrin of **4** leads to a decrease in the amplitude of the excitation spectrum at 456 nm and a corresponding increase at 406 nm, signaling acidification of the liposome interior.

Measurement of the hydrogen ion imbalance across the membrane using pH-sensitive dyes shows that maximum ΔpH values up to ~2 units can be achieved. The transmembrane pH gradient is remarkably stable. When the liposomes are prepared from a suitable mix of phospholipids,[27] the ΔpH is stable for at least 4 h in the dark. Addition of a proton ionophore such as carbonyl cyanide 4-(trifluoromethoxy)phenylhydrazone (FCCP) immediately relaxes the proton gradient.

The proton pumping photocycle transports protons into the liposome interior without translocating any compensating charges. Thus, the pump should develop a transmembrane electrical potential, $\Delta\psi$. Membrane potentials may be detected using the fluorescent dye 8-anilino-1-naphthalenesulfonic acid. When this dye is added to the liposomal proton pumping system, the fluorescence increases in concert with the developing ΔpH, signaling a concurrent buildup of ΔpH and $\Delta\psi$. Both gradients contribute to the pmf, the total potential energy stored by the system. This suggests that if $\Delta\psi$ were relaxed, a larger maximum ΔpH should be achievable. Addition of potassium and valinomycin (a potassium ionophore) to the system reduces $\Delta\psi$ by allowing potassium ions to flow out of the liposome as hydrogen ions are pumped in. Experimentally, relaxing $\Delta\psi$ in this way results in a 1.6-fold increase in the limiting ΔpH. The maximum total free energy conserved by the proton pumping system is on the order of 4 kcal/mol of hydrogen ions. At this value of the pmf, net hydrogen ion translocation across the membrane ceases.

Synthesis of ATP. Proton motive force, generated either by the photosynthetic apparatus or through other electron transport processes in energy-coupling membranes, is the major conduit for biological energy. Although pmf may be used to directly power a variety of processes, the most important application is the endergonic synthesis of ATP from ADP and Pi. This is the case because ATP powers most energy-requiring life processes. Indeed, the human body at rest synthesizes and consumes on the order of 1.5 kg of ATP every hour. Having used photosynthetic principles to design a functional transmembrane light-driven proton pump, it was logical to consider using the pmf to power ATP synthesis.

In photosynthetic membranes and mitochondria, ATP is prepared by ATP synthase enzymes, which consist of a membrane-spanning component (F_0) and a catalytic component projecting into the aqueous phase (F_1). The endergonic synthesis is powered by pmf. Proton flow through the enzyme is coupled to ATP production by a unique "mechanical" mechanism involving rotation of one of the subunits. Thus, the ATP synthase is a molecular-scale rotary motor.

Biochemists have developed procedures for isolating intact ATP synthase molecules and reinserting them into the membranes of liposomes. Using these methodologies, we have vectorially inserted the CF_0F_1-ATP synthase from spinach into the membranes of liposomes and subsequently added the light-driven proton pump.[27] The enzyme is incorporated by adding an aqueous detergent solution of ATP synthase to the preformed liposomes containing quinone **5** and slowly removing the detergent. The enzyme inserts into the membrane as illustrated schematically in Figure 4, with the ATP-producing F_1 subunits on the exterior. Once the enzyme is in place, the triad artificial reaction center is incorporated as described earlier. The liposomal construct is thus set up for light-driven ATP production. The proton pumping photocycle will translocate hydrogen ions into the liposome, establishing a pmf. The enzyme can then transport the protons back out of the liposome, using the pmf to synthesize ATP.

To investigate this possibility, a method for assaying the ATP produced is required. A convenient bioluminescence-based assay uses the firefly luciferin−luciferase system, in which consumption of one molecule of ATP is linked to emission of one photon in the 570-nm region. Alternatively, the reaction may be followed using ^{32}P-labeled ADP and detecting the appearance of the label in the newly synthesized ATP.

Typical results are shown in Figure 6. A solution containing liposomes with the light-driven proton pump and the ATP synthase was prepared, and ATP (0.2 mM), ADP (0.2 mM), and Pi (5 mM) were added. Thioredoxin, which is necessary to activate the enzyme, was also present, and the solution was deaerated. The initial pH was 8.0 on both sides of the membrane. The sample was illuminated with a 5-mW laser at 633 nm, where the porphyrin of **4** absorbs. From time to time, aliquots were

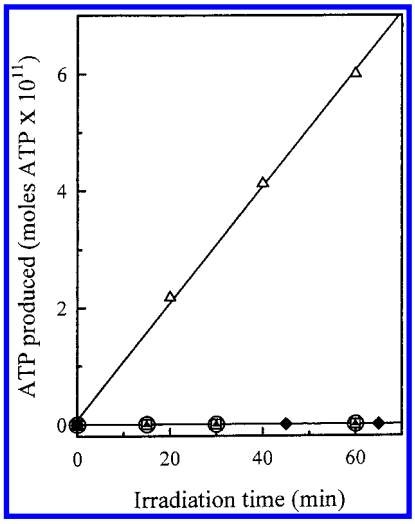

FIGURE 6. Synthesis of ATP by the artificial photosynthetic construct shown in Figure 4 as a function of irradiation time. Also shown are results for control experiments showing that ATP was not synthesized; ○, 1 μM FCCP; ▲, 2 μM tentoxin; ◆, [quinone **5**] = 0; □, [ADP] = 0.

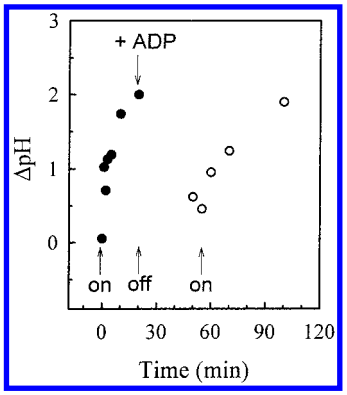

FIGURE 7. In this experiment, the ΔpH produced in the artificial photosynthetic construct shown in Figure 4 was monitored using a pH-sensitive dye. At the beginning of the experiment, all components of the ATP-synthesizing system were present except ADP. Upon irradiation, a ΔpH of ~2 units rapidly developed. It persisted when the actinic light was turned off but was rapidly discharged by the addition of ADP. The gradient was consumed in the production of ATP by ATP synthase. Irradiation was begun again, and the ΔpH was slowly established as the remaining ADP was consumed.

removed and added to an assay solution containing luciferin, luciferase, and buffer. The luminescence spectrum was measured immediately, and the amount of ATP present was determined. Figure 6 shows the amount of ATP produced, relative to a control experiment with an identical but nonilluminated sample.

Also shown in Figure 6 are the results of several control experiments. Addition of FCCP prevents ATP production by abolishing the pmf. Omission of ADP or **5** also eliminates ATP production, as does the addition of 2 μM tentoxin, which is an inhibitor of chloroplast ATP synthase.

The quantum yield of ATP was estimated at low light intensity; one ATP molecule is produced for every 14 incident photons. Because of light scattering by the liposomes, there is some uncertainty in determination of the amount of light absorbed, but spectroscopic measurements suggest that ~50% of the incident light was absorbed by the porphyrin, giving a quantum yield for ATP production of ~0.15. The number of protons transported across the membrane by ATP synthase per ATP molecule produced is the subject of debate and may vary from species to species. Common estimates are three or four protons per ATP. Thus, the quantum yield of proton translocation by the light-driven pump must be in the range 0.5−0.6.

At moderate light levels, the rate of ATP synthesis saturates with respect to light intensity, and the turnover rate of the enzyme may be estimated. Values of more than 100 ATP per second per molecule of ATP synthase can be achieved by the biomimetic system.

The intimate connection between light-driven pmf formation and ATP production in the liposomes is evident from Figure 7. Initially, a liposomal system assembled as described above, but lacking ADP, is irradiated with actinic light. The ΔpH reaches a maximum within a few minutes. The light is turned off, and the proton gradient persists because no substrate for ATP synthase is present. After 20 min, a small amount of ADP is added, and the ΔpH is consumed in the production of ATP. After an additional 30 min, the actinic light is again turned on. The ΔpH rises as residual ADP is converted to ATP, and the ΔpH gradually returns to its maximum value.

Comments and Future Prospects

The liposomal device discussed here is a biomimetic, nanoscale machine capable of converting sunlight into chemical energy. It performs with remarkable efficiency, given its simplicity relative to its biological analogues. The basic functions—harvesting of visible light, energy conversion via multistep photoinduced electron transfer, proton pumping based on a redox loop, and pmf-driven synthesis of high-energy chemicals—are all borrowed from biology but have been reduced to the bare essentials. The fact that the artificial system works at all hints at possible pathways by which photosynthesis could have evolved from abiotic processes. Of course, the photosynthetic, electron-transfer-based solution to the problem of coupling a photochemical process to the formation of a phosphoanhydride bond in ATP is not the only possible approach. Bacteriorhodopsin-based biological solar energy conversion employs a somewhat different, and less universal, method of using light energy to generate pmf.

The system also illustrates that scientific principles and methodologies have advanced to the point that assembly of complex functional nanoscale devices is practical. An overriding principle in the construction of such devices, both natural and artificial, is that of organization. Individual chromophores can absorb light, but energy transfer in an antenna requires suitable electronic interactions among the chromophores, and these in turn are controlled by spatial relationships. Turning to reaction centers, triads **2** and **4** undergo high-yield, rapid, and efficient multistep photoinduced charge separation and slow charge recom-

bination. Achieving this requires molecular engineering such that the desired electron-transfer events are rapid relative to competing processes. Adjusting the electronic coupling between donors and acceptors is crucial to accomplishing this, although energetics and solvation factors are also important. In the model systems described here, the requisite degree of organization is provided by covalent bonds. In natural systems, the protein organizes the various cofactors.

Turning to the next degree of complexity, the liposomal bilayer itself is a marvel of self-assembly. Individual lipid molecules organize to form a bilayer membrane, which in turn achieves a higher degree of order as a closed vesicle. Self-assembly via noncovalent interactions, directed by structural factors designed into the molecules, is responsible for ensuring that the triads and shuttle quinone **5** are incorporated into the bilayer and remain there. Additional organization is required in the form of vectorial insertion of the triad, so that net proton translocation can occur. The ATP synthase is itself a result of several levels of organization—primary, secondary, tertiary, and quaternary structure. Function also requires proper insertion of the F_0 subunit into the membrane, so that proton flow into the liposome can be coupled to proton outflow through the enzyme. Thus, the remarkable thing about the liposomal system described here is not the various components, all of which have precedent, but rather the fact that they can be made to organize themselves into a complex unit capable of carrying out a specific function.

The advent of the transmembrane light-driven proton pump and the ATP-producing liposomal system suggests experiments in which either the pmf or the ATP recycling system could be used to power other processes. Biological applications of pmf include osmotic work and transmembrane metabolite transport, establishment of transmembrane ion gradients, pyrophosphate synthesis, synthesis of reducing equivalents such as NADH and NADPH, and mechanical work such as that done by flagellar motors. Model or biohybrid systems for mimicking these functions are at least theoretically possible. ATP, of course, fuels a large number of enzymatic processes. It is used in large amounts and is rapidly recycled. It may be advantageous to use artificial, light-driven systems to produce ATP in order to carry out enzymatic reactions in the absence of interfering biological materials and without the need for living cells. The fine control of ATP production inherent in a light-driven process offers new possibilities for studying the mechanisms of enzymatic reactions.

Organisms also use ATP to power mechanical motion. As mentioned earlier, the function of ATP synthase involves mechanical rotation of a protein subunit driven by transmembrane proton flux. It is also possible to cause rotation of this subunit via ATP hydrolysis, and this is the basis of some nanoscale biological rotary motors. Linear biological motors such as kinesin and dynein are also powered by ATP. Vesicle systems such as that described above could provide fuel for such biological nanovehicles.

The biologically oriented energy transduction discussed above can lead from light energy to electrochemical potential, to pmf, to ATP, to mechanical motion. This brings to mind the parallel transduction of sunlight to electricity (emf) to mechanical motion via photovoltaic cells and electric motors. Because natural and artificial reaction centers are molecular-scale photovoltaic devices, it is, in principle, possible to incorporate them into electrical circuits. Indeed, chlorophylls and related chromophores can generate electricity via photoinduced electron transfer rather efficiently in dye-sensitized, semiconductor-based photoelectrochemical cells.[28] Interfacing artificial reaction centers with conducting or semiconducting surfaces would allow solar energy conversion and might also have various applications in optoelectronic data manipulation, transmission and storage, and sensor technology. The triad **2** optomagnetic molecular AND gate discussed above illustrates this potential.

The availability of biomimetic artificial photosynthetic nanostructures opens the door to research and possible applications in both the biological realm and the realm of information technology, which has hitherto been dominated by silicon-based devices. This is only one example illustrating that the chemical sciences can fruitfully exploit biology-based ideas and principles to design synthetic constructs that provide the basis for many exciting areas of research and technology.

The authors thank the collaborators, students, and colleagues who have contributed to the research, and whose names are given in the list of references. This work was supported by the U.S. Department of Energy and the National Science Foundation. This is publication 442 from the ASU Center for the Study of Early Events in Photosynthesis.

References

(1) Gould, S. J. *Ever Since Darwin. Reflections in Natural History*; W. W. Norton: New York, 1977; p 91.
(2) Ciamician, G. The photochemistry of the future. *Science* **1912**, *36*, 385−394.
(3) Gust, D.; Moore, T. A. Intramolecular photoinduced electron-transfer reactions of porphyrins. In *The Porphyrin Handbook*; Kadish, K. M., Smith, K. M., Guilard, R., Eds.; Academic Press: New York, 1999; pp 153−190.
(4) Wasielewski, M. R. Photoinduced electron transfer in supramolecular systems for artificial photosynthesis. *Chem. Rev.* **1992**, *92*, 435−461.
(5) Balzani, V.; Moggi, L.; Scandola, F. Towards a supramolecular photochemistry: Assembly of molecular components to obtain photochemical molecular devices. In *Supramolecular Photochemistry*; Balzani, V., Ed.; D. Reidel: Dordrecht, 1987; pp 1−28.
(6) Gust, D.; Moore, T. A.; Moore, A. L. Molecular mimicry of photosynthetic energy and electron transfer. *Acc. Chem. Res.* **1993**, *26*, 198−205.
(7) Meyer, T. J. Chemical approaches to artificial photosynthesis. *Acc. Chem. Res.* **1989**, *22*, 163−170.
(8) Kuciauskas, D.; Liddell, P. A.; Lin, S.; Stone, S.; Moore, A. L.; Moore, T. A.; Gust, D. Photoinduced electron transfer in carotenoporphyrin-fullerene triads: Temperature and solvent effects. *J. Phys. Chem. B* **2000**, *104*, 4307−4321.
(9) Gust, D.; Mathis, P.; Moore, A. L.; Liddell, P. A.; Nemeth, G. A.; Lehman, W. R.; Moore, T. A.; Bensasson, R. V.; Land, E. J.; Chachaty, C. Energy transfer and charge separation in carotenoporphyrins. *Photochem. Photobiol.* **1983**, *37*, S46.
(10) Moore, T. A.; Gust, D.; Mathis, P.; Mialocq, J.-C.; Chachaty, C.; Bensasson, R. V.; Land, E. J.; Doizi, D.; Liddell, P. A.; Lehman, W. R.; Nemeth, G. A.; Moore, A. L. Photodriven charge separation in a carotenoporphyrin-quinone triad. *Nature* (*London*) **1984**, *307*, 630−632.

(11) Liddell, P. A.; Kuciauskas, D.; Sumida, J. P.; Nash, B.; Nguyen, D.; Moore, A. L.; Moore, T. A.; Gust, D. Photoinduced charge separation and charge recombination to a triplet state in a carotene-porphyrin-fullerene triad. *J. Am. Chem. Soc.* **1997**, *119*, 1400−1405.
(12) Carbonera, D.; Di Valentin, M.; Corvaja, C.; Agostini, G.; Giacometti, G.; Liddell, P. A.; Kuciauskas, D.; Moore, A. L.; Moore, T. A.; Gust, D. EPR investigation of photoinduced radical pair formation and decay to a triplet state in a carotene-porphyrin-fullerene triad. *J. Am. Chem. Soc.* **1998**, *120*, 4398−4405.
(13) Gust, D.; Moore, T. A.; Moore, A. L.; Liddell, P. A.; Kuciauskas, D.; Sumida, J. P.; Nash, B.; Nguyen, D. A carotene-porphyrin-fullerene triad: Photoinduced charge separation and charge recombination to a triplet state. In *Recent Advances in the Chemistry and Physics of Fullerenes and Related Materials*, *4*; Kadish, K. M., Rutherford, A. W., Eds.; The Electrochemical Society: Pennington, NJ, 1997; pp 9−24.
(14) Gust, D.; Moore, T. A.; Moore, A. L.; Kuciauskas, D.; Liddell, P. A.; Halbert, B. D. Mimicry of carotenoid photoprotection in artificial photosynthetic reaction centers: Triplet−triplet energy transfer by a relay mechanism. *J. Photochem. Photobiol. B*: *Biol.* **1998**, *43*, 209−216.
(15) Kuciauskas, D.; Liddell, P. A.; Moore, T. A.; Moore, A. L.; Gust, D. Solvent effects and electron-transfer dynamics in a porphyrin-fullerene dyad and a carotenoporphyrin-fullerene triad. In *Recent Advances in the Chemistry and Physics of Fullerenes and Related Materials*, *6*; Kadish, K. M., Ruoff, R. S., Eds.; The Electrochemical Society: Pennington, NJ, 1998; pp 242−261.
(16) Kuciauskas, D.; Liddell, P. A.; Moore, A. L.; Moore, T. A.; Gust, D. Magnetic switching of charge separation lifetimes in artificial photosynthetic reaction centers. *J. Am. Chem. Soc.* **1998**, *120*, 10880−10886.
(17) Dutton, P. L.; Leigh, J. S.; Seibert, M. Primary processes in photosynthesis: *In situ* ESR studies on the light induced oxidized and triplet state of reaction center bacteriochlorophyll. *Biochem. Biophys. Res. Commun.* **1972**, *46*, 406−413.
(18) Thurnauer, M. C.; Katz, J. J.; Norris, J. R. The triplet state in bacterial photosynthesis. Possible mechanisms of the primary photo-act. *Proc. Natl. Acad. Sci. U.S.A.* **1975**, *72*, 3270−3274.
(19) McGann, W. J.; Frank, H. A. Transient electron spin resonance spectroscopy of the carotenoid triplet state in *Rhodopseudomonas sphaeroides* wild type. *Chem. Phys. Lett.* **1985**, *121*, 253−261.
(20) Gust, D. Very small arrays. *Nature* (*London*) **1997**, *386*, 21−22.
(21) Hsiao, J.-S.; Krueger, B. P.; Wagner, R. W.; Johnson, T. E.; Delaney, J. K.; Mauzerall, D. C.; Fleming, G. R.; Lindsey, J. S.; Bocian, D. F.; Donohoe, R. J. Soluble synthetic multiporphyrin arrays. 2. Photodynamics of energy-transfer processes. *J. Am. Chem. Soc.* **1996**, *118*, 11181−11193.
(22) Wagner, R. W.; Lindsey, J. S. A molecular photonic wire. *J. Am. Chem. Soc.* **1994**, *116*, 9759−9760.
(23) Wagner, R. W.; Lindsey, J. S.; Seth, J.; Palaniappan, V.; Bocian, D. F. Molecular optoelectronic gates. *J. Am. Chem. Soc.* **1996**, *118*, 3996−3997.
(24) Kuciauskas, D.; Liddell, P. A.; Lin, S.; Johnson, T. E.; Weghorn; S. J.; Lindsey, J. S.; Moore, A. L.; Moore, T. A.; Gust, D. An artificial photosynthetic antenna-reaction center complex. *J. Am. Chem. Soc.* **1999**, *121*, 8604−8614.
(25) Steinberg-Yfrach, G.; Liddell, P. A.; Hung, S.-C.; Moore, A. L.; Gust, D.; Moore, T. A. Artificial photosynthetic reaction centers in liposomes: Photochemical generation of transmembrane proton potential. *Nature* (*London*) **1997**, *385*, 239−241.
(26) Mitchell, P. Chemiosmotic coupling in oxidative and photosynthetic phosphorylation. *Biol. Rev. Camb. Philos. Soc.* **1966**, *41*, 445−502.
(27) Steinberg-Yfrach, G.; Rigaud, J.-L.; Durantini, E. N.; Moore, A. L.; Gust, D.; Moore, T. A. Light-driven production of ATP catalyzed by F_0F_1-ATP synthase in an artificial photosynthetic membrane. *Nature* (*London*) **1998**, *392*, 479−482.
(28) O'Regan, B.; Grätzel, M. Light-induced redox reactions in nanocrystalline systems. *Nature* (*London*) **1991**, *353*, 737−740.

AR9801301